JOURNAL OF AIRCRAFT
Vol. 32, No. 4, July–August 1995

Natural-Laminar-Flow Airfoil for General-Aviation Applications

Michael S. Selig*
University of Illinois at Urbana–Champaign, Urbana, Illinois 61801
Mark D. Maughmer†
Pennsylvania State University, University Park, Pennsylvania 16802
and
Dan M. Somers‡
Airfoils, Inc., State College, Pennsylvania 16803

A natural-laminar-flow airfoil, the NLF(1)-0115, has been recently designed for general-aviation aircraft at the NASA Langley Research Center. During the design of this airfoil, special emphasis was placed on experiences and observations gleaned from other successful general-aviation airfoils. For example, the flight lift-coefficient range is the same as that of the turbulent-flow NACA 23015 airfoil. Also, although beneficial for reducing drag and producing high lift, the NLF(1)-0115 airfoil avoids the use of aft loading, which can lead to large stick forces if utilized on portions of the wing having ailerons. Furthermore, not using aft loading eliminates the concern that the high pitching-moment coefficient generated by such airfoils can result in large trim drag if cruise flaps are not employed. The NASA NLF(1)-0115 airfoil has a thickness of 15% chord. It is designed primarily for general-aviation aircraft with wing loadings of 720–960 N/m² (15–20 lb/ft²). Low-profile drag as a result of laminar flow is obtained over the range from $c_l = 0.1$ and $R = 9 \times 10^6$ (the cruise condition) to $c_l = 0.6$ and $R = 4 \times 10^6$ (the climb condition). While this airfoil can be used with flaps, it is designed to achieve a $c_{l,\max}$ of 1.5 at $R = 2.6 \times 10^6$ without flaps. The zero-lift pitching moment is held to $c_{m,0} = -0.055$. The hinge moment for a 20% chord aileron is fixed at a value equal to that of the NACA 63_2-215 airfoil, $c_H = -0.0022$. The loss in $c_{l,\max}$ due to leading-edge roughness at $R = 2.6 \times 10^6$ is 11% as compared with 14% for the NACA 23015.

Introduction

WITH increasing use of composite structures in general-aviation aircraft, it is possible to obtain tolerances and levels of surface smoothness such that the use of laminar flow airfoils can result in significant gains in aircraft performance.[1] In the past, many attempts to exploit such airfoils were not completely successful. For example, the loss of the laminar flow due to leading-edge contamination sometimes resulted in a significant reduction in the maximum lift coefficient, which could produce very dangerous situations with regard to take-off and landing. Also causing concern was the fact that some earlier laminar-flow airfoils were aft-loaded in order to have long regions of favorable pressure gradients resulting in significant runs of laminar flow. For some applications, the use of such airfoils can result in trim-drag penalties due to large nose-down pitching moments. Likewise, if such airfoils are used over the regions of the wings in which control surfaces are located, large control forces can exist and the control surfaces can have a tendency to "float."

Using the experience obtained with laminar-flow airfoils over the years, an airfoil has been designed that provides the performance gains possible with laminar flow but without the concerns associated with some of the earlier efforts. The result of this design effort is an airfoil having performance better than those airfoils traditionally used for such applications, while retaining all the desirable characteristics of those older airfoils.

Received Oct. 13, 1993; revision received Nov. 25, 1994; accepted for publication Dec. 8, 1994.

*Assistant Professor, Department of Aeronautical and Astronautical Engineering, 306 Talbot Laboratory, 104 S. Wright St. Member AIAA.

†Associate Professor, Department of Aerospace Engineering, 233 Hammond Bldg. Senior Member AIAA.

‡President, 601 Cricklewood Dr.

Airfoil Design Objectives and Constraints

Many of the design requirements for a modern general-aviation airfoil can be derived from other successful general-aviation airfoils. Most notably, the turbulent-flow NACA 23015 airfoil[2] has been a popular choice for general-aviation applications for many years. This fact stems not only from the broad lift range and low pitching moment, but also from the small loss in $c_{l,\max}$ due to leading-edge contamination. The laminar-flow NACA 63_2-215 airfoil[2] has also had wide appeal owing to its low-drag, although it suffers from a narrow usable lift range as compared with the NACA 23015 airfoil.

The principal goal of the present airfoil-design effort is to maintain the lift range of the NACA 23015 airfoil while realizing low-drag characteristics similar to those of the NACA 63_2-215 airfoil. In particular, low profile drag is desired over the range from $c_l = 0.1$ at $R = 9 \times 10^6$ (the cruise condition) to $c_l = 0.6$ at $R = 4 \times 10^6$ (the climb condition). The Reynolds numbers at each flight condition are typical of general-aviation aircraft with wing loadings in the range 720 to 960 N/m² (15 to 20 lb/ft²). While this airfoil could employ flaps, it is required that without flaps $c_{l,\max} \geq 1.5$ at $R = 2.6 \times 10^6$ (the takeoff/landing condition). In case of leading-edge contamination, the loss in $c_{l,\max}$ should be no larger than 14%, the same as that experienced by the NACA 23015 airfoil. To minimize trim-drag penalties, it is desired that $c_{m,0} > -0.055$. Furthermore, for a control surface of 20% chord (0.2c), the hinge-moment coefficient should be no more negative than that of the NACA 63_2-215 airfoil, $c_H > -0.0022$. In this case stick forces and control surface "float" should not be excessive. Lastly, the airfoil thickness is required to be 15% chord.

NASA NLF(1)-0115 Airfoil

The result of the present design effort is the NASA NLF(1)-0115, shown in Fig. 1 along with three inviscid velocity distributions corresponding to the key flight conditions: cruise, climb, and takeoff/landing. The theoretical section characteristics are shown in Fig. 2 for $R = 9 \times 10^6$ and 4×10^6, the cruise and climb Reynolds numbers, respectively. The section characteristics shown in this and all subsequent figures are predicted with the Eppler code.[3,4] Results predicted by this code have been compared with experiment and show good agreement for airfoils similar to the NLF(1)-0115 over a comparable Reynolds number range.[4-8] Thus, it is anticipated that the predictions would be realized in flight and wind-tunnel tests. The zero-lift pitching-moment and hinge-moment coefficients fall within the design constraints, $c_{m,0} = -0.055$ and $c_H = -0.0022$ for a $0.2c$ control surface. The airfoil thickness is 15% chord, as desired. The airfoil coordinates are given in Table 1.

A comparison between the section characteristics of the NASA NLF(1)-0115 airfoil and those of the NACA 23015 airfoil at the cruise-flight Reynolds number is presented in Fig. 3. The design goal of maintaining a broad lift range similar to that of the NACA 23015 airfoil has been achieved. The low-drag benefit due to laminar flow is achieved over the cruise-flight lift-coefficient range. It should be noted that one

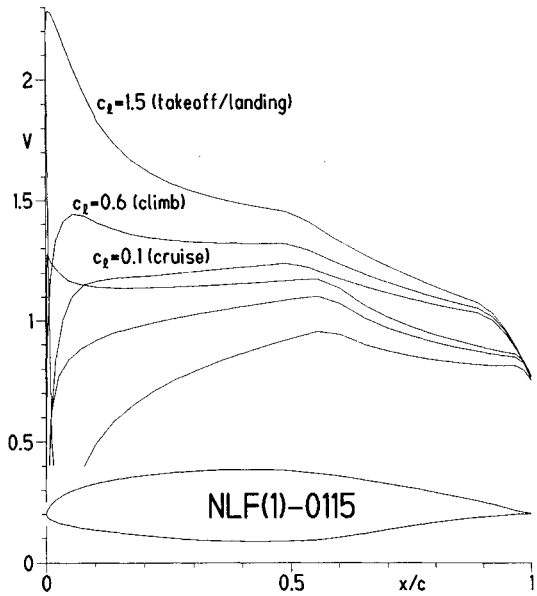

Fig. 1 NASA NLF(1)-0115 airfoil and inviscid velocity distributions.

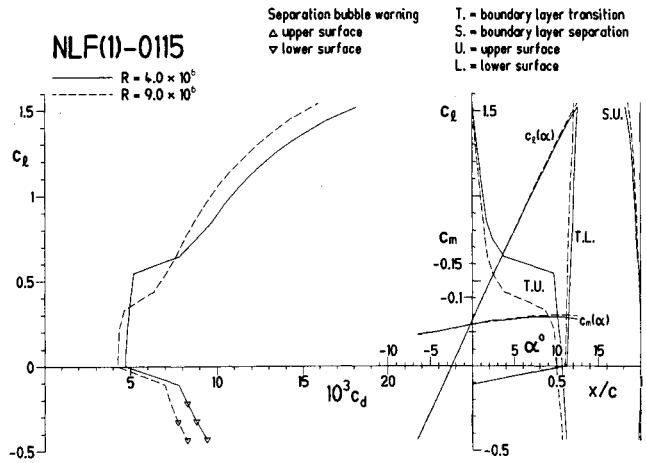

Fig. 2 Theoretical section characteristics of the NASA NLF(1)-0115 airfoil.

Table 1 NLF(1)-0115 airfoil coordinates

Upper surface		Lower surface	
x/c	y/c	x/c	y/c
0.00000	0.00012	0.00252	−0.00715
0.00270	0.00940	0.01126	−0.01302
0.00954	0.01957	0.02600	−0.01859
0.02048	0.02992	0.04634	−0.02384
0.03560	0.03993	0.07192	−0.02889
0.05494	0.04928	0.10230	−0.03376
0.07855	0.05773	0.13698	−0.03841
0.10644	0.06522	0.17547	−0.04279
0.13842	0.07180	0.21723	−0.04681
0.17420	0.07751	0.26171	−0.05036
0.21335	0.08239	0.30835	−0.05333
0.25536	0.08643	0.35657	−0.05558
0.29969	0.08957	0.40578	−0.05698
0.34578	0.09170	0.45539	−0.05733
0.39307	0.09269	0.50482	−0.05642
0.44103	0.09238	0.55345	−0.05373
0.48908	0.09046	0.60155	−0.04844
0.53711	0.08650	0.65013	−0.04101
0.58540	0.08060	0.69911	−0.03297
0.63378	0.07350	0.74738	−0.02532
0.68161	0.06575	0.79388	−0.01850
0.72820	0.05769	0.83761	−0.01278
0.77287	0.04961	0.87762	−0.00828
0.81494	0.04170	0.91305	−0.00497
0.85376	0.03411	0.94313	−0.00274
0.88867	0.02685	0.96722	−0.00133
0.91933	0.01975	0.98498	−0.00042
0.94579	0.01293	0.99613	−0.00004
0.96792	0.00704	1.00000	0.00000
0.98507	0.00282	—	—
0.99614	0.00060	—	—
1.00000	0.00000	—	—

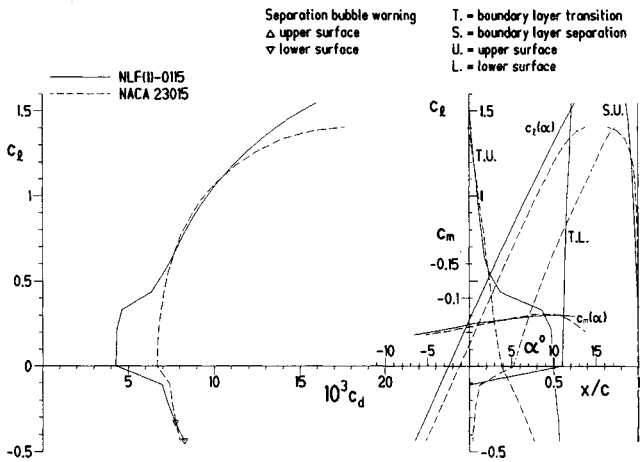

Fig. 3 Comparison of the theoretical section characteristics of the NASA NLF(1)-0115 and NACA 23015 airfoils for $R = 9 \times 10^6$.

of the tradeoffs to be made for the lower drag coefficient is an increase in the nose-down pitching-moment coefficient.

The effects of leading-edge contamination shown in Fig. 4 are for the takeoff/landing Reynolds number of 2.6×10^6. The predicted $c_{l,\max}$ for the NLF(1)-0115 airfoil is not overly sensitive to roughness. In fact, the lift loss due to contamination is only 11% as compared with 14% for the NACA 23015 airfoil.

Design Procedure and Philosophy

Design Methodology

The airfoil design process was carried out using the Eppler Airfoil Design and Analysis Code.[3,4] For design, an inverse method is used to allow for the specification of the velocity

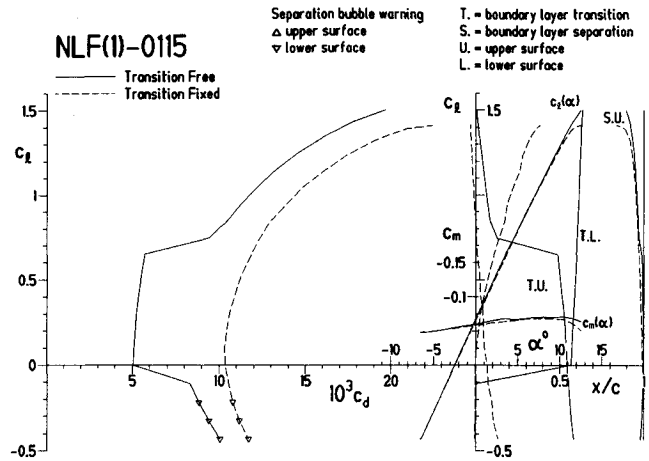

Fig. 4 The effects of leading-edge roughness on the theoretical section characteristics of the NASA NLF(1)-0115 airfoil for $R = 2.6 \times 10^6$.

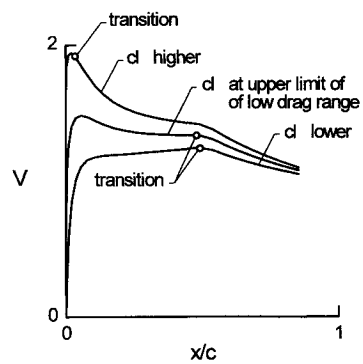

Fig. 5 Behavior of the upper-surface velocity distribution that limits $c_{l,\max}$ sensitivity to leading-edge roughness.

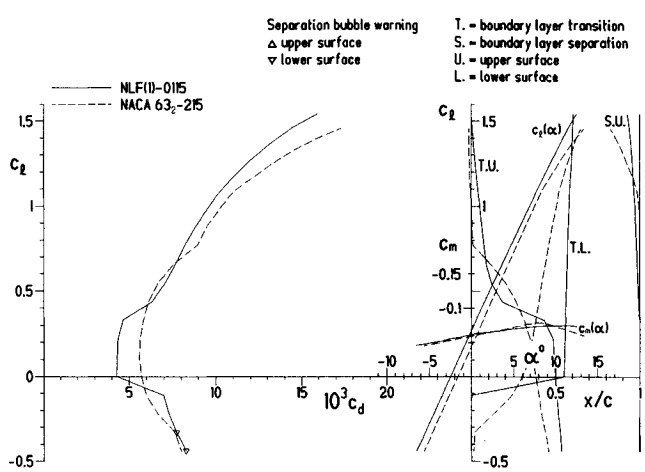

Fig. 6 Comparison of the theoretical section characteristics of the NASA NLF(1)-0115 and NACA 63_2-215 airfoils for $R = 9 \times 10^6$.

distribution from which the airfoil shape is determined. A key feature of the approach (which is based on conformal mapping), is that different segments of the airfoil can be independently designed for different operating conditions. More specifically, the velocity gradient over a segment of the airfoil can be manipulated to achieve a desired boundary-layer development, e.g., a boundary-layer development that sustains laminar flow. For instance, the upper surface can be designed to promote laminar flow at the upper corner of the laminar bucket. Simultaneously, the lower surface can be designed for the lower corner of the laminar bucket. In this way, the desired performance envelope is a consequence of the actual design effort rather than that which is obtained when a point-design airfoil is operated off-design. This multipoint design capabilty is one of the key attributes of the method. In addition to Refs. 3 and 4, the interested reader is directed to Refs. 9 and 10 for a more general discussion of the inverse approach.

Limited Sensitivity to Roughness

In order to have limited sensitivity to leading-edge roughness, the NLF(1)-0115 airfoil embodies upper-surface velocity distributions that behave as generally depicted in Fig. 5. The velocity distribution at $c_l = 0.6$ (the upper limit of the low-drag range for $R = 4 \times 10^6$) is prescribed such that, with increasing angle of attack, the transition point moves rapidly forward to the leading edge from a point just upstream of the main pressure recovery at midchord. Thus, for $c_l < 0.6$, the pressure gradients confine transition to the short "transition ramp" just upstream of the main pressure recovery. For $c_l > 0.6$, the adverse pressure gradient over the forward portion of the airfoil causes transition to occur very near the leading edge. Consequently, because turbulent flow is predominant on the upper surface at $c_{l,\max}$, the maximum lift coefficient is not dramatically influenced by leading-edge roughness.

Achievement of Laminar Flow

In Fig. 6, a comparison is made between the section characteristics of the NASA NLF(1)-0115 and the NACA 63_2-215 airfoils for $R = 9 \times 10^6$. At the cruise condition ($c_l = 0.1$),

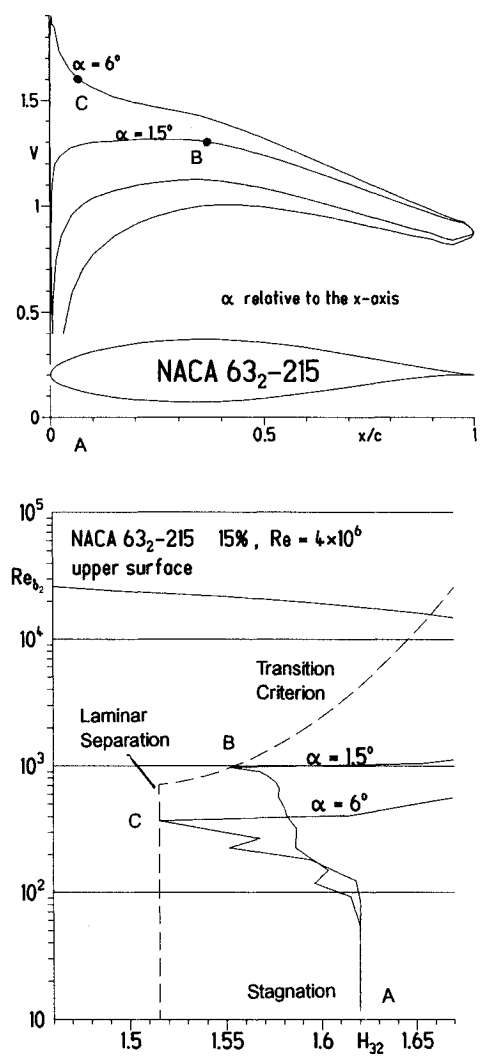

Fig. 7 Theoretical boundary-layer development for the NACA 63_2-215 airfoil surface at $c_l = 0.4$ ($\alpha = 1.5$ deg) and 0.8 ($\alpha = 6$ deg) for $R = 4 \times 10^6$.

the NLF(1)-0115 airfoil has 25% less drag than does the NACA 63_2-215 airfoil, and this advantage is maintained over most of the operational envelope. Although both airfoils are designed to have substantial runs of laminar flow, significant differences exist in the way in which they are achieved. The differences are best interpreted using the theoretical boundary-layer development plot, such as shown in Fig. 7, which requires some preliminary discussion.

In Fig. 7, the local Reynolds number based on the boundary-layer momentum thickness and local velocity R_{δ_2} is plotted against the shape factor based on the energy and momentum thicknesses H_{32}. Note that the logarithmic scale for R_{δ_2} "expands" the boundary-layer development near the leading edge, and "compresses" it downstream. Starting from the stagnation point, R_{δ_2} increases monotonically along the upper surface of the airfoil. Certain values of H_{32} correspond to specific, laminar boundary-layer phenomena. An H_{32} of 1.620 corresponds to stagnation, 1.573 to the flat-plate Blasius boundary layer, and 1.515 to laminar separation. It is noted that H_{32} has the opposite tendency of the perhaps more familiar H_{12}, which contains the displacement thickness rather than the energy thickness. Thus, H_{32}, unlike H_{12}, decreases from stagnation toward laminar separation.

The Eppler method of predicting transition is based on the local values of H_{32} and R_{δ_2}. Within the boundaries given in Fig. 7, the flow is predicted to be laminar. The vertical boundary to the left corresponds to laminar separation ($H_{32} = 1.515$), while the transition-criterion curve corresponds to natural transition. This transition criterion was empirically derived from airfoil wind-tunnel and flight-test data and should therefore be considered as approximate as it is a fairing through the experimental data points. Once transition is predicted, the method switches to the turbulent boundary-layer equations.

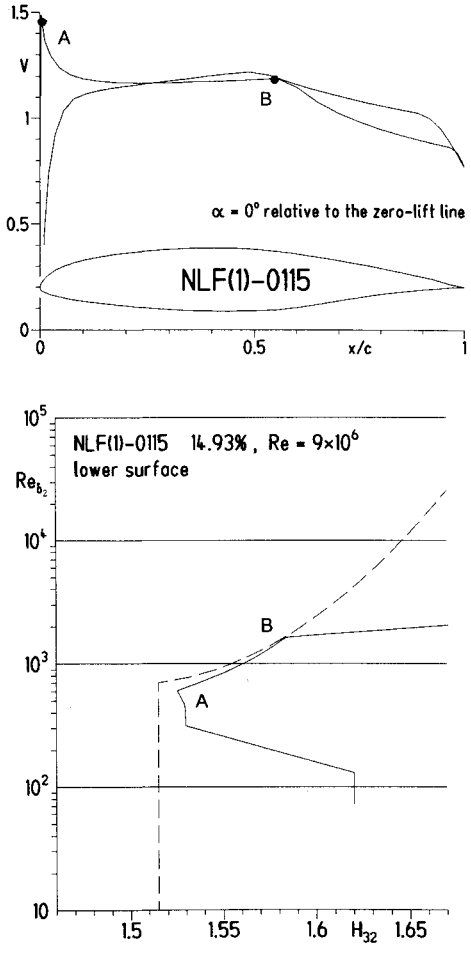

Fig. 8 Theoretical boundary-layer development for the NASA NLF(1)-0115 airfoil lower surface at $c_l = 0$ and $R = 9 \times 10^6$.

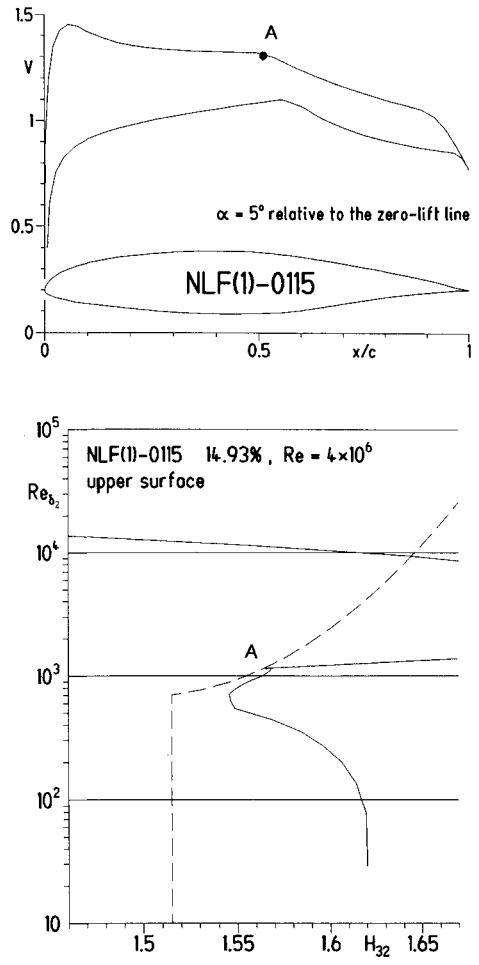

Fig. 9 Theoretical boundary-layer development for the NASA NLF(1)-0115 airfoil upper surface at $c_l = 0.4$ and $R = 4 \times 10^6$.

The two boundary-layer developments shown in Fig. 7 are for the upper surface of the NACA 63_2-215 airfoil at $\alpha = 1.5$ and 6 deg, which corresponds to $c_l = 0.4$ and 0.8, for $R = 4 \times 10^6$. Both boundary-layer developments begin in the lower right at the stagnation point (point A). For $c_l = 0.4$, the curve meets the transition-criterion curve (point B) at which location transition is predicted to occur. As the angle of attack increases, the boundary-layer development curves skew toward the left as the pressure gradients become more adverse. For $c_l = 0.8$, the steep adverse pressure gradient immediately downstream of the velocity peak near the leading edge (point C) results in a more rapid decrease in H_{32} and causes transition via a laminar separation bubble.

When the boundary-layer data are provided in this fashion, they reveal valuable information related to transition and thereby offer clues as to how to sustain laminar flow in the design of an airfoil. For example, referring to Fig. 7 at $c_l = 0.8$, transition is predicted to occur very near the leading edge. If the adverse pressure gradient over this region were reduced, transition would be postponed. By adjusting of the velocity distribution based on the boundary-layer development plot, laminar flow can be extended further back on the airfoil and is limited only by boundary-layer separation or one of the design constraints. As discussed in Ref. 5 and first suggested in Ref. 11, the widest possible low-drag range is achieved when the laminar boundary layer is held on the verge of laminar separation and then on the verge of boundary-layer transition. Such a scenario would be characterized by a boundary-layer development that follows the dotted laminar separation and natural transition boundaries in Fig. 7 (as an ex-

ample, see Figs. 8 and 9 discussed later). While certainly not suitable for all situations and design goals, this concept has been exploited in the design of other airfoils (such as those presented in Refs. 6, 7 and 12) and is now employed in the NLF(1)-0115 airfoil.

Figure 8 shows the boundary-layer development for the lower surface of the NLF(1)-0115 at $c_l = 0.0$ and $R = 9 \times 10^6$, which corresponds to the lower limit of the low-drag range (see Fig. 2). First the laminar-separation limit is approached quickly and is followed for a short distance up to point A. The boundary-layer development then essentially follows the transition-criterion curve. The small distance between the boundary-layer development curve and the transition curve provides a margin for error in the empirical transition criterion as well as in practical application (since the airfoil geometry will not be perfectly reproduced). The beginning of the transition ramp at point B causes the transition criterion to be satisfied, which, in turn, invokes the turbulent boundary-layer calculations.

For the upper surface, the critical design condition occurs at the upper limit of the low-drag range. The corresponding boundary-layer development is shown in Fig. 9 for $c_l = 0.6$ and $R = 4 \times 10^6$. Unlike the design of the lower surface, the upper surface is not designed to rapidly approach laminar separation. Rather, from the stagnation point to $0.1c$, the design of the upper surface is dictated by $c_{l,\max}$ and leading-edge roughness considerations, as previously discussed. From

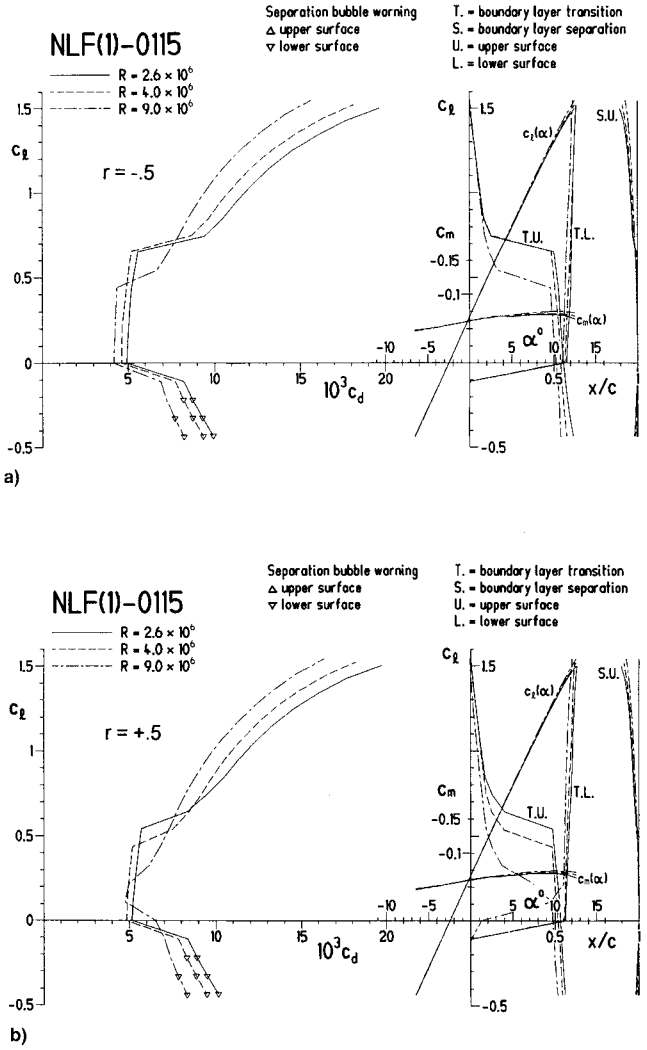

Fig. 10 Theoretical section characteristics for different degrees of roughness: a) decreased roughness: $r = -0.5$ and b) increased roughness: $r = 0.5$.

$0.1c$ to $0.5c$, however, the boundary layer is again forced to be everywhere on the verge of transition.

Although, based on previous experience, the predictions are believed to be fairly accurate, it is nevertheless of interest to investigate the sensitivity of the performance predictions to the transition criterion in order to gain some quantitative understanding of the uncertainty. In particular, the sensitivity of the laminar-bucket width to changes in the momentum-thickness Reynolds number of the transition-criterion curve can be examined by shifting the transition-criterion curve up and down. Before proceeding, it should be stated that the original transition criterion is generally conservative; i.e., transition is more often predicted too early rather than too late.

In the notation used in Ref. 4, Fig. 10a corresponds to a roughness degree r of -0.5, and Fig. 10b is for an r of 0.5. Typically, $r = 4$ correlates well with disturbances caused by an accumulation of insect debris on the airfoil or by the free-stream turbulence observed in many wind tunnels. In Fig. 10a for a reduced degree of roughness ($r = -0.5$), the forward movement of transition on the upper surface is delayed to higher angles of attack. Consequently, the width of the laminar bucket is expanded. Within the bucket, the extent of laminar flow is hardly changed since transition occurs rapidly in the presence of the adverse pressure gradient that begins near midchord on both surfaces. For an increased degree of roughness ($r = 0.5$) shown in Fig. 10b, the opposite effect is observed; the laminar bucket width is contracted. Again, since the original transition curve is conservative, the characteristics shown in Fig. 10b are most likely representative of the onset of insect accumulation or increased wind-tunnel turbulence.

Satisfaction of the Hinge-Moment Constraint

In large part, the airfoil pitching-moment constrains the hinge moment. Nevertheless, some adjustment to the hinge moment is possible through the design of the pressure gradients in the trailing-edge region. In particular, as shown in Fig. 1, a steep adverse pressure gradient begins near 90% chord on the upper surface and near 98% chord on the lower surface. The extent and steepness of these two gradients can be used to achieve the desired hinge moment.

Conclusions

A 15%-thick, natural laminar-flow airfoil designed at NASA Langley Research Center, the NASA NLF(1)-0115, is intended for use in general-aviation applications where high speed and long range are paramount. Incorporated into this design are favorable features derived from several, existing successful airfoils. The desired performance was achieved through careful design of the boundary-layer development, specifically, the movement of the transition location with lift coefficient. For the cruise-flight condition, laminar flow on the lower surface is maintained up to $0.55c$. For the climb condition, laminar flow back to $0.5c$ on the upper surface is predicted. For the takeoff/landing condition, the airfoil is designed so that transition takes place very near the leading edge. Thus, leading-edge contamination caused by rain and bugs should not have much effect since the boundary layer is already turbulent. Consequently, the loss in $c_{l,\max}$ due to roughness is minimized. These features should prove to make the NLF(1)-0115 airfoil successful in application to general-aviation aircraft.

Finally, based on this discussion, it is clear that if the design requirements were altered, the design of a new airfoil would be warranted. For example, if the upper limit of the low-drag range was to occur at $c_l = 0.7$ and $R = 3 \times 10^6$ (rather than at $c_l = 0.6$ and $R = 4 \times 10^6$), this would require modification of the upper-surface velocity distribution while simultaneously keeping within the other constraints. Put simply, for maximum performance, the airfoil should be tailored specifically to the aircraft mission requirements.

Acknowledgments

The support of the NASA Langley Research Center under Grant NGT-50341 is gratefully acknowledged.

References

[1]Holmes, B. J., Obara, C. J., and Yip, L. P., "Natural Laminar Flow Experiments on Modern Airplane Surfaces," NASA TP-2256, June 1984.

[2]Abbott, I. H., and Von Doenhoff, A. E., *Theory of Wing Sections*, Dover, New York, 1959.

[3]Eppler, R., and Somers, D. M., "A Computer Program for the Design and Analysis of Low-Speed Airfoils," NASA TM-80210, August 1980.

[4]Eppler, R., *Airfoil Design and Data*, Springer–Verlag, Berlin, 1990.

[5]Somers, D. M., "Subsonic Natural-Laminar-Flow Airfoils," *Natural Laminar Flow and Laminar Flow Control*, edited by R. W. Barnwell and M. Y. Hussaini, Springer–Verlag, New York, 1992, pp. 143–176.

[6]Somers, D. M., "Design and Experimental Results for a Flapped Natural-Laminar-Flow Airfoil for General Aviation Applications," NASA TP-1865, June 1981.

[7]Maughmer, M. D., and Somers, D. M., "Design and Experimental Results for a High-Altitude, Long-Endurance Airfoil," *Journal of Aircraft*, Vol. 26, No. 2, 1989, pp. 148–153.

[8]Eppler, R., "Turbulent Airfoils for General Aviation," *Journal of Aircraft*, Vol. 15, No. 2, 1978, pp. 93–99.

[9]Selig, M. S., and Maughmer, M. D., "Multipoint Inverse Airfoil Design Method Based on Conformal Mapping," *AIAA Journal*, Vol. 30, No. 5, 1992, pp. 1162–1170.

[10]Selig, M. S., and Maughmer, M. D., "Generalized Multipoint Inverse Airfoil Design," *AIAA Journal*, Vol. 30, No. 11, 1992, pp. 2618–2625.

[11]Eppler, R., "Laminar Airfoils for Reynolds Numbers Greater than 4×10^6," National Technical Information Service, N69-28178, translated from Ingenieur-Archiv, Bd. 38, Heft 4/5, B-819-35, 1969, pp. 232–240.

[12]Somers, D. M., and Horstmann, K. H., "Design of a Medium-Speed, Natural-Laminar-Flow Airfoil for Commuter Aircraft Applications," Inst. fur Entwurfsaerodynamik, IB 129-85/26, Braunschweig, Germany, April 1985.